UDP-*N*-acetylmuramic Acid (UDP-MurNAc) Is a Potent Inhibitor of MurA (Enolpyruvyl-UDP-GlcNAc Synthase)†

Shehadeh Mizyed,‡,§ Anna Oddone,‡ Bartosz Byczynski,‡ Donald W. Hughes,‡ and Paul J. Berti*,‡,||

Departments of Chemistry and Biochemistry and the Antimicrobial Research Centre, McMaster University, 1280 Main Street West, Hamilton, Ontario L8S 4M1, Canada

Received October 27, 2004; Revised Manuscript Received December 27, 2004

ABSTRACT: Purified recombinant MurA (enolpyruvyl-UDP-GlcNAc synthase) overexpressed in *Escherichia coli* had significant amounts of UDP-MurNAc (UDP-*N*-acetylmuramic acid) bound after purification. UDP-MurNAc is the product of MurB, the next enzyme in peptidoglycan biosynthesis. About 25% of MurA was complexed with UDP-MurNAc after five steps during purification that should have removed it. UDP-MurNAc isolated from MurA was identified by mass spectrometry, NMR analysis, and comparison with authentic UDP-MurNAc. Subsequent investigation showed that UDP-MurNAc bound to MurA tightly, with $K_{d,UDP-MurNAc} = 0.94 \pm 0.04$ μM, as determined by fluorescence titrations using ANS (8-anilino-1-naphthalenesulfonate) as an exogenous fluorophore. UDP-MurNAc binding was competitive with ANS and phosphate, the second product of MurA, and it inhibited MurA. The inhibition patterns were somewhat ambiguous, likely being competitive with the substrate PEP (phosphoenolpyruvate) and either competitive or noncompetitive with respect to the substrate UDP-GlcNAc (UDP-*N*-acetylglucosamine). These results indicate a possible role for UDP-MurNAc in regulating the biosynthesis of nucleotide precursors of peptidoglycan through feedback inhibition. Previous studies indicated that UDP-MurNAc binding to MurA was not tight enough to be physiologically relevant; however, this was likely an artifact of the assay conditions.

The cytoplasmic phase of peptidoglycan biosynthesis has been studied extensively, but significant questions remain about its regulation (*1*−*4*). The first committed step of peptidoglycan biosynthesis is catalyzed by MurA (EP-UDP-GlcNAc synthase)[1] (*2*). It transfers the enolpyruvyl moiety of phosphoenolpyruvate (PEP) to UDP-*N*-acetylglucosamine (UDP-GlcNAc), forming enolpyruvyl-UDP-*N*-acetylglucosamine (EP-UDP-GlcNAc) and inorganic phosphate (P_i) (Figure 1). MurA is an antimicrobial target, being irreversibly inhibited by the antibiotic fosfomycin (*5*, *6*). Its mechanism (*7*−*14*) and structure (*6*, *15*) have been characterized extensively.

In the next step, MurB reduces EP-UDP-GlcNAc to UDP-*N*-acetylmuramic acid (UDP-MurNAc). Six more cytoplasmic steps complete synthesis of UDP-MurNAc-pentapeptide (*16*). An undecaprenyl pyrophosphate carrier lipid and UDP-GlcNAc are added at the cell membrane, followed by transfer to a final acceptor in the expanding peptidoglycan wall.

Peptidoglycan synthesis is tightly regulated (*16*). The mechanism of regulating synthesis of nucleotide precursors of peptidoglycan, including UDP-MurNAc-pentapeptide, appears to involve controlling the entry of precursors into the biosynthetic pathway. It is not clear how this is achieved, but feedback inhibition by a variety of peptidoglycan precursors has been suggested (*1*, *4*). Regulation does not appear to be achieved by controlling enzyme levels, as they appear to be constitutively expressed and are relatively insensitive to a wide variety of conditions (*17*). For example, MurA levels in fosfomycin-treated *Salmonella typhimurium* were unaffected by the antibiotic over a range of concentrations (*18*). EP-UDP-GlcNAc concentrations are low, ca. 2 μM (*19*), and remarkably constant under a wide variety of conditions in wild-type strains, implying tight regulation (*17*).

We report here that purified recombinant MurA contained significant amounts of bound UDP-MurNAc after purification, suggesting a possible physiological role for this interaction. We have shown that UDP-MurNAc is a MurA inhibitor.

MATERIALS AND METHODS

General. Fosfomycin, PEP, and UDP-GlcNAc were purchased from Sigma. [^{33}P]PEP was prepared from [γ-^{33}P]ATP as described previously (*20*, *21*).

MurB. The strain expressing His_6-tagged MurB was the generous gift of Dr. Martin Pavelka (University of Roches-

† This work was supported by the Canadian Institutes of Health Research, as well as by a graduate scholarship from the Natural Sciences and Engineering Research Council of Canada (to B.B.).

* To whom correspondence should be addressed. Telephone: (905) 525-9140 ext 23479. Fax: (905) 522-2509. E-mail: berti@mcmaster.ca.

‡ Department of Chemistry, McMaster University.

§ Present address: Department of Chemistry, Yarmouk University, Irbid, Jordan.

|| Department of Biochemistry, McMaster University.

[1] Abbreviations: ANS, 8-anilino-1-naphthalenesulfonate; DTT, dithiothreitol; EP-UDP-GlcNAc, enolpyruvyluridine diphospho *N*-acetylglucosamine; $K_{d,X}$, equilibrium dissociation constant of compound X binding with MurA; MurA, EP-UDP-GlcNAc synthase; MurB, EP-UDP-GlcNAc reductase; PEP, phosphoenolpyruvate; P_i, inorganic phosphate; TOCSY, total correlation spectroscopy; TLC, thin-layer chromatography; UDP-GlcNAc, uridine diphospho *N*-acetylglucosamine; UDP-MurNAc, uridine diphospho *N*-acetylmuramic acid; UDP-MurNAc-pentapeptide, UDP-*N*-acetylmuramyl-L-Ala-D-Glu-*meso*-diaminopimelic acid-D-Ala-D-Ala.

10.1021/bi047704w CCC: $30.25
Published on Web 02/16/2005

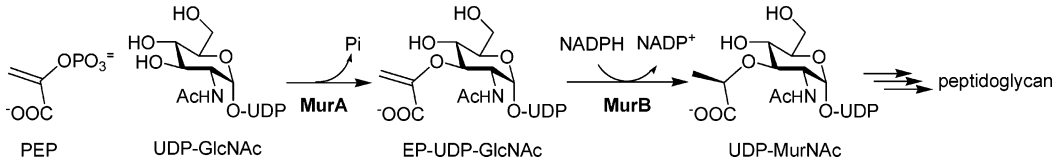

FIGURE 1: The first two cytoplasmic steps of peptidoglycan biosynthesis.

ter). It was expressed and purified as described previously (*22*), except that Ni^{2+}-affinity purification was chromatographic rather than batchwise.

MurA. *Escherichia coli* MurA was overexpressed and purified as described previously (*23*). Protein concentrations were determined using $\epsilon_{280} = 13250\ M^{-1}\ cm^{-1}$, and the concentration of active MurA was determined by titrating its activity with fosfomycin (*24*). For these assays, MurA activity was measured by detecting the appearance of P_i spectrophotometrically using ammonium molybdate/Malachite Green dye (*25*).

Extensive dialysis of purified MurA against 50 mM Tris-HCl, pH 7.5, 1 mM DTT, 1 mM phenylmethanesulfonyl fluoride, and 1 mM EDTA at 4 °C overnight increased the size of the change in the fluorescence signal in titrations with UDP-MurNAc (data not shown) without affecting $K_{d,UDP-MurNAc}$ (apparent), suggesting that an unknown, low molecular weight species with modest affinity for MurA was being removed during dialysis.

Covalent MurA Adduct. The presence of the covalent hemithioketal adduct of PEP to MurA (*26*, *27*) was investigated by converting it to EP-UDP-GlcNAc. UDP-GlcNAc (8 μM) was combined with 4 μM MurA for 30 min in 200 μL of 50 mM Tris-HCl, pH 7.5, and 1 mM DTT at room temperature, followed by quenching with 0.1 M KOH and quantitating EP-UDP-GlcNAc by HPLC (*23*).

UDP-MurNAc. UDP-MurNAc was prepared from UDP-GlcNAc, PEP, and NADPH using MurA and MurB. A 2.0 mL reaction mixture contained 25 mM PEP, 15 mM UDP-GlcNAc, 15 mM KCl, 75 mM Tris-HCl, pH 7.5, 5 mM DTT, and 100 μM MurA. After incubation for 6 h at 37 °C, 20 mM NADPH and 15 μM MurB were added, and the reaction proceeded for 20 h longer. The reaction progress was monitored by HPLC anion-exchange chromatography with a Mono-Q column (1 mL, Amersham Biosciences), with a gradient of 100−500 mM KCl in 10 mM NH_4Cl, pH 10.0, over 30 min, at 1 mL/min, with A_{260} detection. UDP-MurNAc was purified by anion-exchange and reverse-phase HPLC after the enzymes were removed by ultrafiltration. The filtered reaction mixture was applied to an anion ion-exchange column (20 mL of Q-Sepharose, Amersham Biosciences) with a gradient of 500−750 mM ammonium acetate, pH 9.0, over 15 min at 5 mL/min, and then stepping to 1.0 M over 3 min, with A_{260} detection. UDP-MurNAc eluted at ca. 15.5 min. It was further purified by C18 reverse-phase chromatography with isocratic elution in 2% MeOH: 98% 50 mM Et_3NHOAc, pH 6.0, at 1.0 mL/min, with A_{260} detection. The UDP-MurNAc peak was collected, diluted with H_2O, and lyophilized several times to remove the volatile buffer salts and then stored at −20 °C. The overall yield was 83%.

Structure Determinations. UDP-MurNAc was isolated from purified MurA by denaturing 50 mg of MurA (700 μL, 1.6 mM) with 0.2 M KOH. The quenched reaction mixture was extracted repeatedly with chloroform to precipitate and remove protein, followed by ultrafiltration to complete protein removal. UDP-MurNAc was purified on a Mono-Q anion-exchange column (1 mL, Amersham Biosciences) with a gradient of 100−500 mM ammonium bicarbonate, pH 10, over 15 column volumes at 0.5 mL/min flow rate and A_{260} detection. Both UDP-MurNAc isolated from MurA and authentic UDP-MurNAc were analyzed by mass spectrometry and NMR. ^1H NMR spectra were recorded on a Bruker Avance 600 MHz NMR spectrometer. The spectra were obtained at 22 °C in 40 scans in 64K data points over a 8.091 kHz spectral width (4.050 s acquisition time). The residual HDO solvent peak was suppressed by presaturation during the 1.5 s relaxation delay between acquisitions. A pulse width of 5.95 μs (90° flip angle) was used. Free induction decays were processed using exponential multiplication with 0.2 Hz line broadening and zero-filling to 128K before Fourier transformation. Selective 1-D TOCSY ^1H NMR spectra with pulsed field gradients were recorded under similar conditions, with selective excitation by a Gaussian-shaped pulse with a 180° pulse width of 83.4 ms. This pulse was followed by the standard TOCSY MLEV-17 spin-lock pulse sequence (*28*). The 90° spin-lock pulse width was 63.0 μs, the relaxation delay was 1.0 s, the spin-lock period was 100 ms, and the transmitter offset was adjusted to the frequency of the ^1H being selectively excited. The spectrum was acquired in 160 scans. The free induction decays were processed as above. ^1H chemical shifts were determined relative to the HDO signal at 4.80 ppm as an internal reference. Authentic UDP-MurNAc and material isolated from MurA were dissolved in 99.9% D_2O (Cambridge Isotope Labs, Inc.) at concentrations of approximately 10 and 1 mM, respectively.

ANS Fluorescence Titrations. The dissociation equilibrium constant, $K_{d,UDP-MurNAc}$, was determined using fluorescence titrations with the fluorescent probe 8-anilino-1-naphthalenesulfonate (ANS). ANS associates with MurA (*12*), which increases its fluorescence relative to unbound ANS (λ_{ex} =366 nm, λ_{em} = 500 nm). Ligands that displaced ANS from MurA typically resulted in a 10−15% decrease in fluorescence, although the decrease was about 80% in the presence of >10 mM phosphate (data not shown). $K_{d,UDP-GlcNAc}$, as determined by fluorescence titration in this study, was 52 ± 11 μM (data not shown) and was in good agreement with the previously reported value, 59 ± 6 μM (*14*), as was the value of $K_{d,ANS}$, 36 ± 9 μM, determined indirectly in this study (see Results section), compared with the literature value of 41 ± 3 μM (*12*).

Fluorescence titrations were typically performed with 3 μM MurA and 100 μM ANS in 50 mM Tris-HCl, pH 7.5, and 1 mM DTT, in 2.0 mL at 20 °C, with continuous stirring. Some titrations used 1 μM MurA and 33 μM ANS or 5 μM MurA and 200 μM ANS; [MurA] was varied to maintain a ratio of ANS:MurA between 33 and 66 (*12*). Samples were thermally equilibrated for ca. 45 min, until the fluorescence was stable, then UDP-MurNAc aliquots were added, and the

fluorescence was read at 1 and 5 min after each addition to ensure stable readings. Control samples were titrated with water in parallel. Raw fluorescence readings were corrected for dilution. Titrations were also performed in the presence of 2−20 mM potassium phosphate. Titrating 100 μM ANS with P_i in the presence or absence of 3 μM MurA showed no significant changes in fluorescence.

Fluorescence titration data were fitted to equations that either accounted for (eq 1) or neglected (eq 2) the binding of ANS:

$$F = F_0 - (F_0 - F_{inf}) \times \left(\frac{[\text{UDP-MurNAc}]}{K_{d,\text{UDP-MurNAc}}\left(1 + \frac{[\text{ANS}]}{K_{d,\text{ANS}}}\right) + [\text{UDP-MurNAc}]} \right) \quad (1)$$

$$F = F_0 - (F_0 - F_{inf}) \times \left(\frac{[\text{UDP-MurNAc}]}{K_{d,\text{UDP-MurNAc}}(\text{apparent}) + [\text{UDP-MurNAc}]} \right) \quad (2)$$

where F is the observed fluorescence, F_0 and F_{inf} are the fitted values for fluorescence at zero and infinite UDP-MurNAc concentrations, $K_{d,\text{UDP-MurNAc}}$ is the fitted equilibrium dissociation constant for UDP-MurNAc, $K_{d,\text{UDP-MurNAc}}$ (apparent) is the apparent value when the effect of ANS binding is neglected, and $K_{d,\text{ANS}}$ is the previously determined dissociation equilibrium constant for ANS binding to MurA, 41 μM (*12*).

$K_{d,\text{UDP-MurNAc}}$ was also determined from plots of $K_{d,\text{UDP-MurNAc}}$(apparent) versus a competitive ligand, L, namely, ANS or P_i (eq 3):

$$K_{d,\text{UDP-MurNAc}}(\text{apparent}) = K_{d,\text{UDP-MurNAc}}\left(1 + \frac{[\text{L}]}{K_{d,\text{L}}}\right) \quad (3)$$

$K_{d,\text{UDP-MurNAc}}$ was the *y*-intercept upon linear extrapolation to [L] = 0, and $K_{d,\text{L}}$ was the *y*-intercept/slope.

Inhibition. Reaction rates were determined by following the conversion of [^{33}P]PEP to [^{33}P]phosphate by anion-exchange thin-layer chromatography (TLC) on poly(ethylenimine)−cellulose, with 2 M sodium acetate, pH 5.0, as solvent and detection of radioactivity by storage phosphor autoradiography (*21*, *29*). Reaction rates at 25 °C were determined using 0−16 μM UDP-MurNAc with 50 nM MurA, 50−400 μM UDP-GlcNAc, and 400−1200 nM PEP in 50 mM NH_4HCO_3, pH 7.5, and 0.1 mg/mL bovine serum albumin, with 4000−6000 cpm of ^{33}P per time point, and reaction times of 1−10 min. At each time point, a 10 μL aliquot was quenched with 2 μL of 2 N trifluoroacetic acid, lyophilized, and resuspended in 2 μL of H_2O, and 1 μL was applied to the TLC plate. Initial velocities were determined in the linear part of the [P_i] versus time curve, with [P_i] calculated from the relative intensities of the P_i and PEP spots.

RESULTS

UDP-MurNAc Complexed with Recombinant MurA. Recombinant *E. coli* MurA was expressed with purified yields of 40−75 mg/L of culture, as described previously (*23*). Initial preparations contained UDP-MurNAc in stoichiometries of ca. 0.25 relative to MurA even though each of the five purification and concentration steps should have removed low molecular weight compounds. In later preparations, extensive washing during hydrophobic interaction chromatography (>5 column volumes) lowered the stoichiometry of UDP-MurNAc below 0.1 relative to MurA.

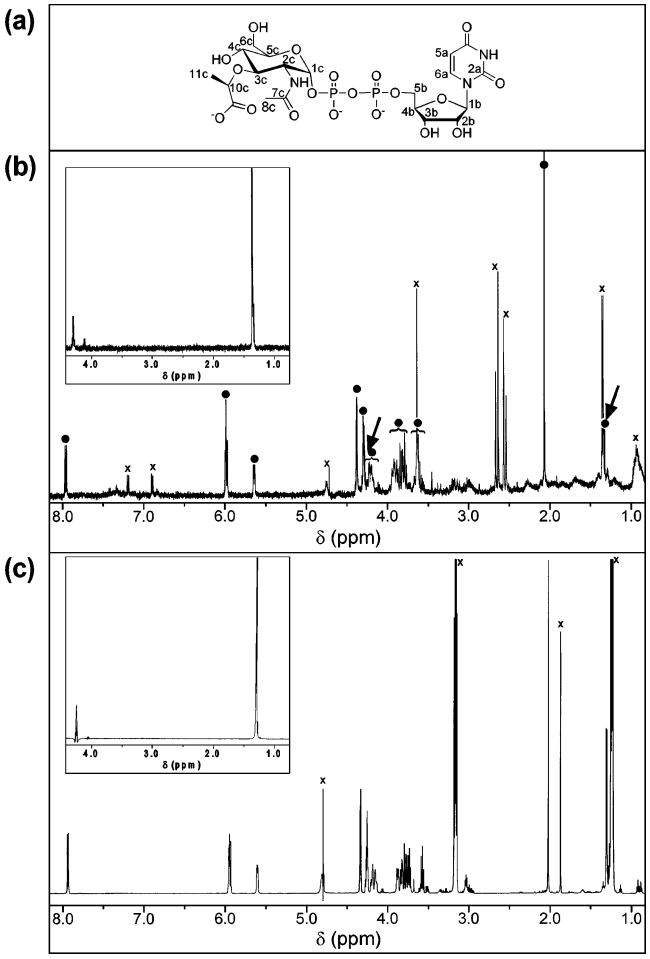

FIGURE 2: ^{1}H NMR spectra of UDP-MurNAc. (a) Structure of UDP-MurNAc showing atom numbering. (b) UDP-MurNAc as isolated from MurA: (●) peaks assigned to UDP-MurNAc; (x) contaminant, solvent, or buffer peaks. (c) Authentic UDP-MurNAc synthesized enzymatically. (Insets) 1-D TOCSY spectra showing through-bond coupling of H11c (1.35 ppm, right arrow in main panel) with H10c (4.29 ppm, left arrow).

Scheme 1

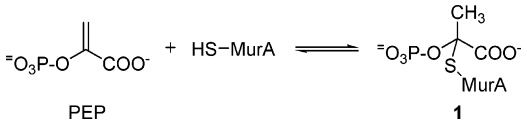

PEP Adduct. Previously, MurA was isolated as a covalent adduct of PEP (**1**, Scheme 1) with a stoichiometry of 1.0 (*26*) or 0.1−0.2 (*27*). It is not on the normal catalytic pathway but is catalytically competent, producing EP-UDP-GlcNAc upon addition of UDP-GlcNAc (*26*). In this study, **1** was present with stoichiometries of up to 0.07. Presumably, UDP-MurNAc binding and **1** are mutually exclusive.

Structure of UDP-MurNAc. UDP-MurNAc isolated from MurA had a molecular weight by negative ion mass spectrometry of m/z_{obs} = 678.1 (m/z_{calc} = 678.4) and had the same retention time on Mono-Q anion-exchange chromatography as authentic UDP-MurNAc. The NMR spectrum agreed with the authentic UDP-MurNAc (Figure 2), as well

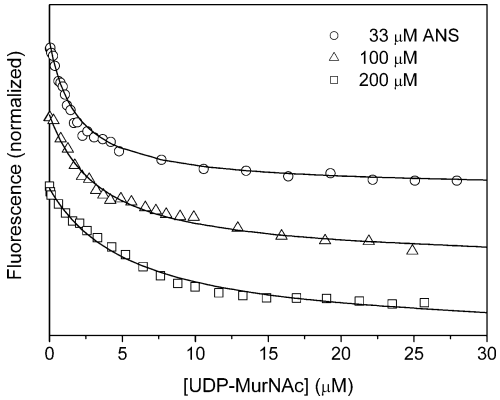

FIGURE 3: UDP-MurNAc titration of MurA with varying [ANS]. [MurA] was varied to maintain ANS:MurA ratios of 33−66. Key: (○) 33 μM ANS, 1 μM MurA; (△) 100 μM ANS, 3 μM MurA; (□) 200 μM ANS, 5 μM MurA.

as the literature spectrum of UDP-MurNAc (*30*), with all chemical shifts within 0.03 ppm of the reported values. The peaks for protons 2b and 3b were overlapped, but the multiplet at 4.38 ppm agreed with the literature chemical shifts of 4.37 and 4.36 ppm. There were contaminants in UDP-MurNAc isolated from MurA, so selective 1-D TOCSY was used to confirm that protons 10c and 11c was coupled (Figure 2, inset).

Determining $K_{d,UDP-MurNAc}$. The dissociation constant of UDP-MurNAc with MurA was determined by fluorescence titration with ANS. The value of $K_{d,UDP-MurNAc}$(apparent), fitted to eq 2, was sensitive to ANS concentration, increasing as ANS increased (Figure 3). This indicated competitive binding between UDP-MurNAc and ANS.[2] Similarly, $K_{d,UDP-MurNAc}$(apparent) increased in the presence of P_i, the second product of MurA, indicating that UDP-MurNAc and P_i binding were also competitive.

Three approaches were used to extract the intrinsic value of $K_{d,UDP-MurNAc}$. Fitting the fluorescence data directly to eq 1, which takes into account ANS binding, yielded $K_{d,UDP-MurNAc} = 0.97 \pm 0.06$ μM. As expected, this value did not vary with [ANS]. Determining $K_{d,UDP-MurNAc}$(apparent) at 33−200 μM ANS and extrapolating to [ANS] = 0 gave $K_{d,UDP-MurNAc} = 0.90 \pm 0.16$ μM (Figure 4a). Similarly, $K_{d,UDP-MurNAc}$(apparent) versus [P_i] was extrapolated to $K_{d,UDP-MurNAc} = 0.94 \pm 0.18$ μM. The "best" value of $K_{d,UDP-MurNAc}$ was taken as the mean of these three values, i.e., 0.94 ± 0.04 μM. Using eq 3 yielded $K_{d,ANS}$, 36 ± 9 μM, within experimental error of the literature value, 41 ± 3 μM (*12*), and $K_{d,P_i} = 1.8 \pm 0.6$ mM, within experimental error of the literature value of $K_{M,P_i} = 2.1$ mM (*31*).

Inhibition by UDP-MurNAc. UDP-MurNAc binding inhibited MurA activity. Because of difficulties in determining the absolute value of the inhibition constant, $K_{i,UDP-MurNAc}$, only the patterns of inhibition were determined; i.e., competitive versus noncompetitive versus uncompetitive. Measuring $K_{i,UDP-MurNAc}$ would be possible if the substrate K_M's were accurately known. However, $K_{M,PEP}$[3] has been reported to be 200 nM (*31*), 400 nM (*34*), or 4.1 μM (*35*). The combination of exceedingly slow reactions at low substrate concentrations and the need to use extents of reaction <10% to obtain the linear part of the progress curve made attaining the needed sensitivity for rate determinations very difficult. This was partially overcome by using a ^{33}P-based assay, combined with performing reactions in volatile buffer, and then concentrating aliquots by lyophilization before TLC.

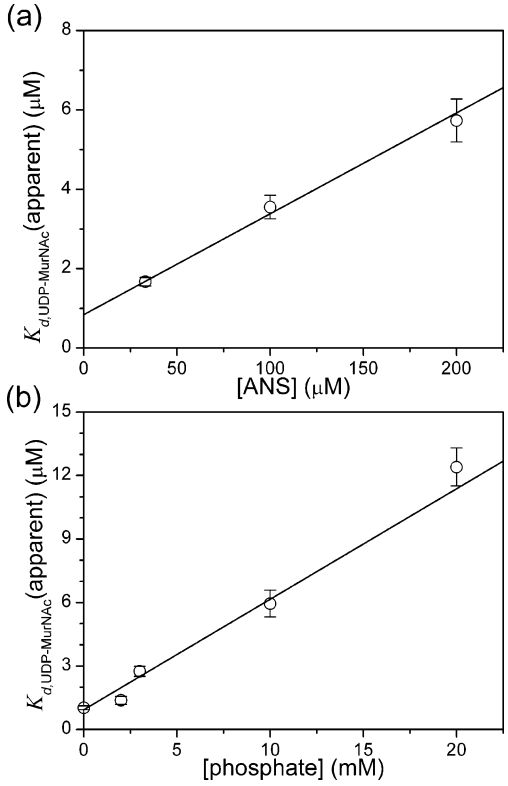

FIGURE 4: Competitive binding: $K_{d,UDP-MurNAc}$(apparent) versus [ANS] and [P_i]. MurA was titrated with UDP-MurNAc in the presence of (a) 33−200 μM ANS, fitted to eq 2, or (b) 0−20 mM P_i and 100 μM ANS, fitted to eq 1.

For both UDP-GlcNAc and PEP, initial velocities were determined at varying UDP-MurNAc concentrations with one substrate concentration held fixed and the other varied. Replotting initial velocities in a Dixon plot (*36*), i.e., $1/v_0$ versus [UDP-MurNAc], would give parallel lines for uncompetitive inhibition, which was not observed (Figure 5). The fact that the lines intersected indicated either competitive or noncompetitive inhibition. In a Dixon plot, the distinction between competitive and noncompetitive inhibition is whether the lines intersect at the *x*-axis or above it. The difficult assay conditions made the intersection points ambiguous. The inhibition pattern with respect to PEP appeared to give intersection above the *x*-axis, possibly indicating competitive rather than noncompetitive inhibition against PEP. The inhibition pattern with respect to UDP-GlcNAc was not clear, and it was not possible to distinguish competitive versus noncompetitive binding based on the Dixon plot. Noncompetitive inhibition requires that both UDP-MurNAc and the substrates bind simultaneously with the enzyme. This seems unlikely given the fact that binding is competitive against P_i

[2] Competitive binding is often interpreted to indicate that two ligands binding to the protein occupy the same physical space, but the more general definition is that binding of those two ligands is mutually exclusive, even if the binding sites are physically distinct.

[3] The fact that $K_{M,PEP}$ is so much lower than $K_{d,PEP}$ suggests highly cooperative substrate binding, as observed in the related enzyme, AroA (*32*, *33*), and/or partially irreversible substrate binding. When both UDP-GlcNAc and PEP concentrations are low, the cooperative effect is lost and reaction rates drop dramatically, making them effectively unmeasurable.

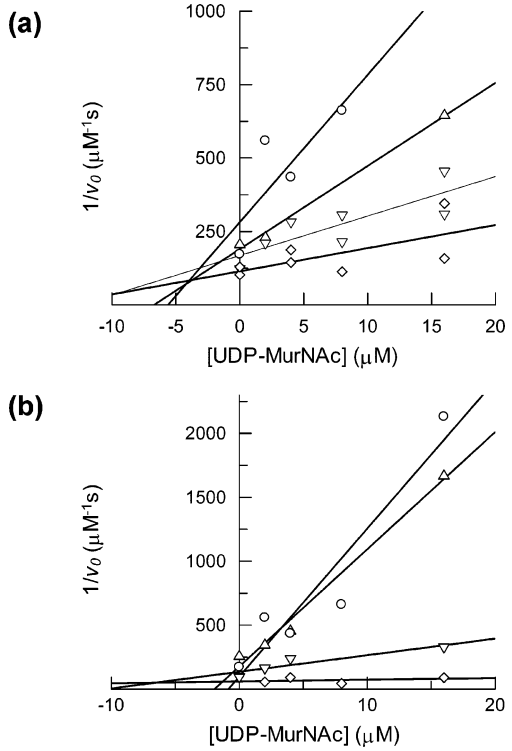

FIGURE 5: Dixon plots of patterns of inhibition by UDP-MurNAc. (a) With respect to PEP, reactions contained 50 nM MurA, 50 μM UDP-GlcNAc, and PEP: (○) 400 nM, (△) 600 nM, (▽) 800 nM, or (◇) 1200 nM. (b) With respect to UDP-GlcNAc, reactions contained 50 nM MurA, 400 nM PEP, and UDP-GlcNAc: (○) 50 μM, (△) 100 μM, (▽) 200 μM, or (◇) 400 μM.

and ANS and the similarity of the UDP-MurNAc structure to UDP-GlcNAc and EP-UDP-GlcNAc.

DISCUSSION

UDP-MurNAc Interaction with MurA. UDP-MurNAc binding was competitive with ANS, evidence that it bound close to, or in, the active site. ANS binds near the "hinge" of a loop that closes over the active site during catalysis (*12*). UDP-GlcNAc and PEP cause the loop to close, displacing ANS into solution, where its fluorescence is quenched. It is likely that, like UDP-GlcNAc and PEP, UDP-MurNAc induces loop closure and displaces ANS. UDP-MurNAc binding was also competitive with P_i, the second product of MurA, further evidence for binding in or near the active site. The best estimate of $K_{d,UDP-MurNAc}$ was 0.94 ± 0.04 μM, much tighter than either substrate: $K_{d,UDP-GlcNAc} = 59$ μM, and $K_{d,PEP} = 240$ μM (*14*).

Inhibition by UDP-MurNAc. While fluorescence titrations demonstrated that UDP-MurNAc bound to MurA, rate assays were required to demonstrate that it was an inhibitor. The inhibition pattern versus PEP was most consistent with competitive inhibition (Figure 5), indicating binding in the active site. The inhibition pattern versus UDP-GlcNAc was ambiguous and may have been competitive or noncompetitive.

UDP-MurNAc Binding Site. UDP-MurNAc differs from EP-UDP-GlcNAc by only two hydrogen atoms and only by a 3′-lactoyl group from UDP-GlcNAc. It likely binds in the same position and orientation as UDP-GlcNAc and EP-UDP-GlcNAc. However, an X-ray crystal structure will be necessary to definitively show the binding site.

Assay Conditions Can Affect Putative Feedback Inhibitors. UDP-MurNAc (*37*) and several UDP-MurNAc-peptides (*38*) were examined previously as feedback inhibitors of MurA. The reported inhibition constants were in the multimillimolar range, far above physiological levels, and therefore not physiologically relevant. However, the concentrations of UDP-GlcNAc and PEP were also in the multimillimolar range and also much higher than physiological (*17*, *19*, *39*−*41*). Under these assay conditions, the putative inhibitors were out-competed by high substrate concentrations, especially PEP. For example, in one study, 5 mM UDP-MurNAc gave only 36% inhibition (*38*) because of very high concentrations of both substrates, with 20 mM UDP-GlcNAc 400-fold higher than $K_{d,UDP-GlcNAc}$ and 0.12 mM PEP 30−600-fold higher than $K_{M,PEP}$ (*31*, *34*, *35*). As both substrates appear to compete with UDP-MurNAc, but not with each other, they would combine to prevent inhibition by UDP-MurNAc. In the same study, UDP-MurNAc-pentapeptide gave 78% inhibition of MurA (*38*). Given the fact that we show that $K_{d,UDP-MurNAc} = 0.94$ μM, it is possible that $K_{d,UDP-MurNAc-pentapeptide}$ is much less than 1 μM and that it is also a potent feedback inhibitor of MurA.

Physiological Relevance for Feedback Inhibition. In vivo concentrations of UDP-GlcNAc and PEP are in the range of 100 μM in exponentially growing cells (*19*, *40*, *41*), compared with UDP-MurNAc concentrations around 5−37 μM (*39*). These levels vary with different growth conditions, and PEP occasionally reaches millimolar levels. Under a wide variety of conditions, the ratio of UDP-GlcNAc to UDP-MurNAc varied between 1.7:1 and 11:1 (*42*). Given the fact that UDP-MurNAc binds MurA 60-fold more tightly than UDP-GlcNAc, UDP-MurNAc could inhibit MurA activity, at least partially, under physiological conditions, depending on the PEP concentration.

Is it reasonable to compare a strain expressing 75 mg/L MurA to a wild-type strain or to draw conclusions about wild-type physiology? In the overexpressing strain, intracellular MurA reached ca. 0.5 mM and would produce unusual amounts of EP-UDP-GlcNAc. This would lead to UDP-MurNAc and feedback inhibition of MurA. With 25% of the overexpressed MurA complexed with UDP-MurNAc (likely much higher, depending on how much UDP-MurNAc was lost during protein purification), the intracellular UDP-MurNAc concentration was at least 125 μM. This is much higher than $K_{d,UDP-MurNAc}$ and higher than normal (*39*), implying that it was responding to the high MurA concentration.

Feedback inhibition of MurA is intuitively reasonable. It is the first committed step of peptidoglycan biosynthesis, and inhibition here would prevent unproductive consumption of UDP-GlcNAc, which is a precursor in other metabolic pathways. The existing evidence on regulation of peptidoglycan biosynthesis is consistent with regulation of MurA activity, including the fact that EP-UDP-GlcNAc concentrations in wild-type *E. coli* are low, around 2 μM, and remarkably constant under all conditions examined (*19*), implying (i) tight control and (ii) that it is not itself involved in regulating peptidoglycan biosynthesis. Temperature-sensitive mutants that accumulate EP-UDP-GlcNAc are known (*43*−*45*), but these represent disruptions in the regulation mechanism and are likely not relevant to wild-type *E. coli*.

UDP-MurNAc inhibition of MurA would be only one facet of regulation. UDP-MurNAc can inhibit GlmU, the last enzyme in UDP-GlcNAc synthesis (*46*). Both UDP-MurNAc and UDP-GlcNAc levels decrease in stationary phase, implicating additional control mechanisms (*17*). Gram-positive bacteria may use different regulatory mechanisms, based on different patterns of nucleotide intermediate accumulation in *Staphylococcus aureus* (*47*) and the observed proteolysis of one of the two MurAs in *Bacillus subtilis* (*48*).

CONCLUSIONS

Recombinant *E. coli* MurA was purified with tightly bound UDP-MurNAc, which was isolated and characterized by mass spectrometry and NMR. UDP-MurNAc is the product of MurB, the next enzyme in the peptidoglycan biosynthesis pathway. Authentic UDP-MurNAc was synthesized and shown to bind to MurA with $K_{d,UDP-MurNAc} = 0.94 \pm 0.04$ μM by fluorescence titration. Binding was competitive with ANS, the fluorophore, as well as phosphate, the second product of MurA. Inhibition patterns showed that UDP-MurNAc was a competitive or noncompetitive inhibitor against both substrates, UDP-GlcNAc and PEP. The observed tight binding, combined with the fact that UDP-MurNAc was copurified with MurA from *E. coli*, suggests that it could act as a feedback inhibitor of MurA in regulating peptidoglycan biosynthesis in vivo. This is consistent with the existing literature on the regulation of peptidoglycan biosynthesis.

ACKNOWLEDGMENT

The *E. coli* strain overexpressing His_6-tagged MurB was the generous gift of Prof. Martin Pavelka (University of Rochester). We thank Shaun Lee for technical assistance and Dr. Kirk Green for assistance with mass spectroscopy.

REFERENCES

1. Tipper, D. J., and Wright, A. (1979) in *The Bacteria* (Sokatch, J. R., and Onrnston, L. N., Eds.) p 291, Academic Press, New York.
2. van Heijenoort, J. (1994) in *Bacterial Cell Wall* (Ghuysen, J.-M., and Hakenbeck., R., Eds.) pp 39−54, Elsevier Science B.V., Amsterdam.
3. van Heijenoort, J. (1996) in *Escherichia coli and Salmonella: Cellular and Molecular Biology* (Neidhardt, F. C., Curtis, J. J., III, Ingraham, J. L., Lin, E. C. C., Low, K. B., Magasanik, B., Rezniko., W. S., Riley, M., Schaechter, M., and Umbarger, H. E., Eds.) pp 1025−1034, ASM Press, Washington, DC.
4. van Heijenoort, J. (2001) Recent advances in the formation of the bacterial peptidoglycan monomer unit, *Nat. Prod. Rep. 18*, 503−519.
5. Hendlin, D., Stapley, E. O., Jackson, M., Wallick, H., Miller, A. K., Wolf, F. J., Miller, T. W., Chaiet, L., Kahan, F. M., Foltz, E. L., Woodruff, H. B., Mata, J. M., Hernandez, S., and Mochales, S. (1969) Phosphonomycin, a new antibiotic produced by strains of streptomyces, *Science 166*, 122−123.
6. Schonbrunn, E., Sack, S., Eschenburg, S., Perrakis, A., Krekel, F., Amrhein, N., and Mandelkow, E. (1996) Crystal structure of UDP-*N*-acetylglucosamine *enol*pyruvyltransferase, the target of the antibiotic fosfomycin, *Structure 4*, 1065−1075.
7. Gunetileke, K. G., and Anwar, R. A. (1968) Biosynthesis of uridine diphospho-*N*-acetylmuramic acid. II. Purification and properties of pyruvate-uridine diphospho-*N*-acetylglucosamine transferase and characterization of uridine diphospho-*N*-acetylenopyruvylglucosamine, *J. Biol. Chem. 243*, 5770−5778.
8. Marquardt, J. L., Siegele, D. A., Kolter, R., and Walsh, C. T. (1992) Cloning and sequencing of *Escherichia coli* murZ and purification of its product, a UDP-*N*-acetylglucosamine *enol*pyruvyl transferase, *J. Bacteriol. 174*, 5748−5752.
9. Marquardt, J. L., Brown, E. D., Walsh, C. T., and Anderson, K. S. (1993) Isolation and structural elucidation of a tetrahedral intermediate in the UDP-*N*-acetylglucoamine enolpyruvyl transferase enzymatic pathway, *J. Am. Chem. Soc. 115*, 10398−10399.
10. Lees, W. J., and Walsh, C. T. (1995) Analysis of the enol ether transfer catalyzed by UDP-GlcNAc *enol*pyruvyl transferase using (*E*)- and (*Z*)-isomers of phospho*enol*butyrate: Stereochemical, partitioning, and isotope effect studies, *J. Am. Chem. Soc. 117*, 7329−7337.
11. Samland, A. K., Jelesarov, I., Kuhn, R., Amrhein, N., and Macheroux, P. (2001) Thermodynamic characterization of ligand-induced conformational changes in UDP-*N*-acetylglucosamine *enol*pyruvyl transferase, *Biochemistry 40*, 9950−9956.
12. Schonbrunn, E., Eschenburg, S., Luger, K., Kabsch, W., and Amrhein, N. (2000) Structural basis for the interaction of the fluorescence probe 8-anilino-1-naphthalene sulfonate (ANS) with the antibiotic target MurA, *Proc. Natl. Acad. Sci. U.S.A. 97*, 6345−6349.
13. Schonbrunn, E., Eschenburg, S., Krekel, F., Luger, K., and Amrhein, N. (2000) Role of the loop containing residue 115 in the induced-fit mechanism of the bacterial cell wall biosynthetic enzyme MurA, *Biochemistry 39*, 2164−2173.
14. Schonbrunn, E., Svergun, D. I., Amrhein, N., and Koch, M. H. (1998) Studies on the conformational changes in the bacterial cell wall biosynthetic enzyme UDP-*N*-acetylglucosamine *enol*pyruvyltransferase (MurA), *Eur. J. Biochem. 253*, 406−412.
15. Eschenburg, S., Kabsch, W., Healy, M. L., and Schonbrunn, E. (2003) A new view of the mechanisms of UDP-*N*-acetylglucosamine *enol*pyruvyl transferase (MurA) and 5-*enol*pyruvylshikimate-3-phosphate synthase (AroA) derived from x-ray structures of their tetrahedral reaction intermediate states, *J. Biol. Chem. 278*, 49215−49222.
16. Ishiguro, E. E., and Ramey, W. D. (1978) Involvement of the relA gene product and feedback inhibition in the regulation of UDP-*N*-acetylmuramyl-peptide synthesis in *Escherichia coli*, *J. Bacteriol. 135*, 766−774.
17. Mengin-Lecreulx, D., and van Heijenoort, J. (1985) Effect of growth conditions on peptidoglycan content and cytoplasmic steps of its biosynthesis in *Escherichia coli*, *J. Bacteriol. 163*, 208−212.
18. Kahan, F. M., Kahan, J. S., Cassidy, P. J., and Kropp, H. (1974) Mechanism of action of fosfomycin (phosphonomycin), *Ann. N.Y. Acad. Sci. 235*, 364−386.
19. Mengin-Lecreulx, D., Flouret, B., and van Heijenoort, J. (1983) Pool levels of UDP-*N*-acetylglucosamine and UDP-*N*-acetylglucosamine-*enol*pyruvate in *Escherichia coli* and correlation with peptidoglycan synthesis, *J. Bacteriol. 154*, 1284−1290.
20. Roossien, F. F., Brink, J., and Robillard, G. T. (1983) A simple procedure for the synthesis of [^{32}P]phospho*enol*pyruvate via the pyruvate kinase exchange reaction at equilibrium, *Biochim. Biophys. Acta 760*, 185−187.
21. Mizyed, S., Wright, J. E. I., Byczynski, B., and Berti, P. J. (2003) Identification of the catalytic residues of AroA (*enol*pyruvylshikimate 3-phosphate synthase) using partitioning analysis, *Biochemistry 42*, 6986−6995.
22. Raymond, J. B., Price, N. P., and Pavelka, M. S. (2003) A method for the enzymatic synthesis and HPLC purification of the peptidoglycan precursor UDP-*N*-acetylmuramic acid, *FEMS Microbiol. Lett. 229*, 83−89.
23. Byczynski, B., Mizyed, S., and Berti, P. J. (2003) Nonenzymatic breakdown of the tetrahedral (α-carboxyketal phosphate) intermediates of MurA and AroA, two carboxyvinyl transferases. Protonation of different functional groups controls the rate and fate of breakdown, *J. Am. Chem. Soc. 125*, 12541−12550.
24. Marquardt, J. L., Brown, E. D., Lane, W. S., Haley, T. M., Ichikawa, Y., Wong, C. H., and Walsh, C. T. (1994) Kinetics, stoichiometry, and identification of the reactive thiolate in the inactivation of UDP-GlcNAc *enol*pyruvoyl transferase by the antibiotic fosfomycin, *Biochemistry 33*, 10646−10651.
25. Lanzetta, P. A., Alvarez, L. J., Reinach, P. S., and Candia, O. A. (1979) An improved assay for nanomole amounts of inorganic phosphate, *Anal. Biochem. 100*, 95−97.
26. Brown, E. D., Marquardt, J. L., Lee, J. P., Walsh, C. T., and Anderson, K. S. (1994) Detection and characterization of a phospholactoyl-enzyme adduct in the reaction catalyzed by UDP-*N*-acetylglucosamine enolpyruvoyl transferase, MurZ, *Biochemistry 33*, 10638−10645.
27. Cassidy, P. J., and Kahan, F. M. (1973) A stable enzyme-phospho*enol*pyruvate intermediate in the synthesis of uridine-5′-diphospho-*N*-acetyl-2-amino-2-deoxyglucose 3-*O*-enolpyruvyl ether, *Biochemistry 12*, 1364−1374.

28. Bax, A., and Davis, D. G. (1985) MLEV-17-based two-dimensional homonuclear magnetization transfer spectroscopy, *J. Magn. Reson. 65*, 355−360.
29. Parra, F. (1982) A simple enzymic method for the synthesis of [^{32}P]phospho*enol*pyruvate, *Biochem. J. 205*, 643−645.
30. El Zoeiby, A., Sanschagrin, F., Darveau, A., Brisson, J. R., and Levesque, R. C. (2003) Identification of novel inhibitors of *Pseudomonas aeruginosa* MurC enzyme derived from phage-displayed peptide libraries, *J. Antimicrob. Chemother. 51*, 531−543.
31. Marquardt, J. L. (1993) Ph.D. Thesis, Department of Biological Chemistry and Molecular Pharmacology, Harvard University, Cambridge, MA, p 187.
32. Gruys, K. J., Walker, M. C., and Sikorski, J. A. (1992) Substrate synergism and the steady-state kinetic reaction mechanism for EPSP synthase from *Escherichia coli*, *Biochemistry 31*, 5534−5544.
33. Gruys, K. J., Marzabadi, M. R., Pansegrau, P. D., and Sikorski, J. A. (1993) Steady-state kinetic evaluation of the reverse reaction for *Escherichia coli* 5-*enol*pyruvoylshikimate-3-phosphate synthase, *Arch. Biochem. Biophys. 304*, 345−351.
34. Kim, D. H., Lees, W. J., Kempsell, K. E., Lane, W. S., Duncan, K., and Walsh, C. T. (1996) Characterization of a Cys115 to Asp substitution in the *Escherichia coli* cell wall biosynthetic enzyme UDP-GlcNAc *enol*pyruvyl transferase (MurA) that confers resistance to inactivation by the antibiotic fosfomycin, *Biochemistry 35*, 4923−4928.
35. Dai, H. J., Parker, C. N., and Bao, J. J. (2002) Characterization and inhibition study of MurA enzyme by capillary electrophoresis, *J. Chromatogr. B 766*, 123−132.
36. Cornish-Bowden, A. (1976) *Principles of Enzyme Kinetics*, Butterworths, London.
37. Wickus, G. G., and Strominger, J. L. (1973) Partial purification and properties of the pyruvate-uridine diphospho-*N*-acetylglucosamine transferase from *Staphylococcus epidermidis*, *J. Bacteriol. 113*, 287−290.
38. Venkateswaran, P. S., Lugtenberg, E. J., and Wu, H. C. (1973) Inhibition of phospho*enol*pyruvate:uridine diphosphate *N*-acetylglucosamine *enol*pyruvyltransferase by uridine diphosphate *N*-acetylmuramyl peptides, *Biochim. Biophys. Acta 293*, 570−574.
39. Mengin-Lecreulx, D., Flouret, B., and van Heijenoort, J. (1982) Cytoplasmic steps of peptidoglycan synthesis in *Escherichia coli*, *J. Bacteriol. 151*, 1109−1117.
40. Lowry, O. H., Carter, J., Ward, J. B., and Glaser, L. (1971) The effect of carbon and nitrogen sources on the level of metabolic intermediates in *Escherichia coli*, *J. Biol. Chem. 246*, 6511−6521.
41. Hogema, B. M., Arents, J. C., Bader, R., Eijkemans, K., Yoshida, H., Takahashi, H., Aiba, H., and Postma, P. W. (1998) Inducer exclusion in *Escherichia coli* by non-PTS substrates: the role of the PEP to pyruvate ratio in determining the phosphorylation state of enzyme IIAGlc, *Mol. Microbiol. 30*, 487−498.
42. Mengin-Lecreulx, D., Siegel, E., and van Heijenoort, J. (1989) Variations in UDP-*N*-acetylglucosamine and UDP-*N*-acetylmuramyl-pentapeptide pools in *Escherichia coli* after inhibition of protein synthesis, *J. Bacteriol. 171*, 3282−3287.
43. Matsuzawa, H., Matsuhashi, M., Oka, A., and Sugino, Y. (1969) Genetic and biochemical studies on cell wall peptidoglycan synthesis in *Escherichia coli* K-12, *Biochem. Biophys. Res. Commun. 36*, 682−689.
44. Lugtenberg, E. J., De Haas-Menger, L., and Ruyters, W. H. (1972) Murein synthesis and identification of cell wall precursors of temperature-sensitive lysis mutants of *Escherichia coli*, *J. Bacteriol. 109*, 326−335.
45. Miyakawa, T., Matsuzawa, H., Matsuhashi, M., and Sugino, Y. (1972) Cell-wall peptidoglycan mutants of *Escherichia coli* K12. Existence of two clusters of genes, mra and mrb, for cell-wall peptidoglycan biosynthesis, *J. Bacteriol. 112*, 950−958.
46. Mengin-Lecreulx, D., and van Heijenoort, J. (1994) Copurification of glucosamine-1-phosphate acetyltransferase and *N*-acetylglucosamine-1-phosphate uridyltransferase activities of *Escherichia coli*: characterization of the glmU gene product as a bifunctional enzyme catalyzing two subsequent steps in the pathway for UDP-*N*-acetylglucosamine synthesis, *J. Bacteriol. 176*, 5788−5795.
47. Good, C. M., and Tipper, D. J. (1972) Conditional mutants of *Staphylococcus aureus* defective in cell wall precursor synthesis, *J. Bacteriol. 111*, 231−241.
48. Kock, H., Gerth, U., and Hecker, M. (2004) MurA, catalysing the first committed step in peptidoglycan biosynthesis, is a target of Clp-dependent proteolysis in *Bacillus subtilis*, *Mol. Microbiol. 51*, 1087−1102.

BI047704W